Near-surface domain structures in uniaxially stressed $SrTiO_3$

1998 J. Phys.: Condens. Matter 10 2817

(http://iopscience.iop.org/0953-8984/10/13/002)

J. Phys.: Condens. Matter **10** (1998) 2817–2827. Printed in the UK PII: S0953-8984(98)88041-7

Near-surface domain structures in uniaxially stressed $SrTiO_3$

Jutta Chrosch and Ekhard K H Salje

University of Cambridge, Department of Earth Sciences and IRC in Superconductivity, Downing Street, Cambridge CB2 3EQ, UK

Received 1 October 1997, in final form 11 December 1997

Abstract. Weak uniaxial stress (<1 kPa) along the cubic [100] and [110] directions of $SrTiO_3$ modifies significantly the domain structure near the crystal surface on cooling to the tetragonal phase. High-resolution x-ray rocking curves show that {110} oriented slabs have a preference of '*c*' domains perpendicular to a small (001) surface. On heating from 10 K the domain population increasingly randomizes when the transition point is approached. In {100} oriented slabs the domain population is more random with little temperature dependence for nominally stress-free samples. Uniaxial stress along ⟨001⟩ increases the population of '*a*' domains for $T \rightarrow T_c$. The '*c*' domains have characteristically shorter length scales perpendicular to the surface than the larger '*a*' domains. The rocking angle of '*c*' domains has a much larger angular spread (ca 1°) than those of '*a*' domains.

1. Introduction

$SrTiO_3$ undergoes a multicritical phase transition [1–5] with an $n = 3$-fold degenerate R_{25} soft mode. Accordingly, the transition is traditionally described within the scheme of an $n = 3$ Heisenberg-type effective Hamiltonian and a cubic anisotropic part which characterizes the cubic soft mode dispersion [6]. Uniaxial stress lifts the degeneracy of the order parameter and an $n = 2 \rightarrow n = 1$ crossover behaviour has been observed for uniaxial stress along [100] [7] and along [110] [8]. The splitting of the multicritical point was observed for uniaxial stress along the cubic [111] axis [9]. In both experiments the relevant stresses were in the order of some MPa. Much weaker stress along [110] was needed to modify the temperature evolution of the excess entropy at $T \rightarrow T_c$ [10]. This latter experiment was based on the measurement of the specific heat of a thin slab of $SrTiO_3$ embedded between two pistons which exerted the uniaxial stress. It appeared very likely, therefore, that the evolution of the order parameter and the relevant microstructures can be modified even under very weak stress fields, at least in near-surface parts of the crystal. In this paper we show that this hypothesis is, indeed, correct.

The second motivation for this study stems from the observation that the coherence length scaling at $T > T_c$ is different inside the bulk of a crystal from that near the surface of $SrTiO_3$ [11–17]. Similar experiments are hard to perform at $T < T_c$ because the diffuse x-ray or neutron scattering due to fluctuations is difficult to separate from Bragg scattering of the underlying tetragonal crystal structure. In this study we use the Bragg reflections to analyse one crucial aspect of the microstructures close to the crystal surface, namely the correlation between the three components of the order parameter each of which corresponds to one specific domain orientation. Inside a domain the order parameter is non-degenerate

0953-8984/98/132817+11$19.50

($n = 1$) while $n = 3$ behaviour requires the flipping of domain structures on an atomic scale. We shall argue that such $n = 3$ behaviour might exist in a small temperature interval very close to T_c while large domains develop at temperatures just below T_c.

2. Experimental details

Single crystals of Verneuil grown $SrTiO_3$ in two different orientations, {100} and {110}, were supplied by Crystal GmbH (Berlin). They were cut, ground and polished by the suppliers; the sample size was $1 \times 5 \times 10$ mm^3 with the largest face remaining parallel to (100) or (110).

The x-ray diffraction measurements were conducted using a novel high-resolution instrument where a focused and strictly monochromatic Cu Kα_1 beam is diffracted by the specimen and registered by either a 120° (2θ) position sensitive detector (120-PSD) or an area detector [18–20]. The 2θ resolution was set to 0.03°; all other angular steps were 0.01°. The versatility of the instruments which operate over a temperature range between 5 K and 1100 K has previously been demonstrated in a variety of experiments including the collection of diffuse scattering from domain walls and the determination of extended microstructures [21–24]. In all these cases the measurements were conducted using an x-ray spot size of <100 μm thus minimizing the beam divergence and other instrumental influences. Test experiments with Si-crystals show typical rocking curve widths of 0.02°. The data were analysed by constructing rocking curves by either integrating the diffraction pattern along the 2θ direction or, for 3D diffraction diagrams, simultaneously along 2θ and χ. Alternatively, the diffraction patterns were integrated in the ω direction for constant values of 2θ and χ, respectively. For details of the diffraction geometries we refer the reader to [18].

Two different series of experiments were performed on the {100} and {110} single crystals of $SrTiO_3$. Reflections 400 and 220 from the respective largest face were measured at room temperature by simultaneously translating the sample parallel to the tilt axis [001] in both cases. The diffraction signals were recorded with the area detector and rocking curves (intensity versus ω) were constructed by simultaneously integrating the intensities in 2θ and χ around each reflection. In addition, the measured intensities were analysed in reciprocal space yielding a three-dimensional iso-intensity distribution around the main Bragg reflections. From the former procedure information about the quality of the crystal such as mosaic spread and other angular variations can be obtained, while the latter operation gives a direct indication of the spatial distribution of internal strains [35]. In all cases the penetration depth of the x-ray beam is of the order of at maximum 15 μm so that all observations can be related to the near-surface regions only.

In a second set of experiments the crystals were clamped between two anvils and cooled down to 10 K (figure 1). The temperature was then increased in steps of 2 K up to room temperature. At each temperature a rocking curve was recorded with an angular step size of 0.01°. Due to the geometry of the anvils and for better comparison reflection 004 with $2\theta \approx 105°$ was observed in both the {100} and {110} sample by diffracting from the (001) face. The external stress was applied along the [100] and the [110] directions. The spectra were integrated in 2θ and ω and the resulting peaks fitted with either Gaussian or Lorentzian functions to obtain the position, width and area of the rocking curves and diffraction peaks. The temperature range was in all cases 10 K to 300 K, external stresses were varied between zero and $\approx$1 kPa.

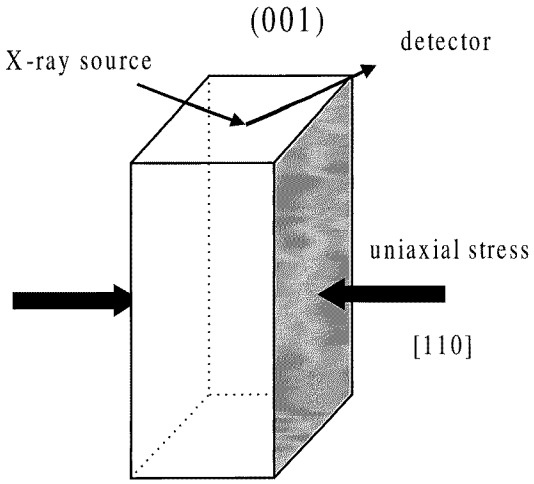

Figure 1. Schematic plot of the sample arrangement. A thin slab of $SrTiO_3$ is squeezed between two anvils and mounted inside a cryostat. The smallest surface on top of the crystal is used for x-ray diffraction; the rocking axis is perpendicular to the face in front of the drawing.

3. Results

3.1. {110} orientation

The results of the room-temperature scan across the (110) face are shown in figure 2. The dominant effect is the bending of the surface which results in peak shifting and even peak splitting in the centre of the large face. Translating the sample across the whole distance of 3.2 mm changes the peak position of 0.08° which is equivalent to a bending radius of ≈2.3 m.

In figure 3 (circles) the rocking peak height ratios $I_{004}/(I_{400} + I_{040} + I_{004})$ are plotted as a function of temperature for three different stresses. The height ratios are quite constant at low pressures and do not vary much with temperature at $T \ll T_c$. On approaching the transition temperature the population of '*a*' domains increases. This effect is strongly stress dependent. Figure 3 (squares) also shows the temperature dependence of the total diffraction intensity for three uniaxial stresses. In all cases a dominance of '*c*' domains is observed.

The angular splitting between the two diffraction peaks of the rocking curve is proportional to the spontaneous strain of the phase transition, $e_{1,sp} = (a(T) - a_0)/a_0$ and $e_{2,sp} = (c(T) - a_0)/a_0$, where $a(T)$ and $c(T)$ are the lattice parameters at the temperature T and a_0 is the lattice parameter of the cubic phase extrapolated to the same temperature (for definitions of ferroelastic strains see [31]). The spontaneous strain scales in lowest-order theory as the square of the order parameter with the effective temperature exponent β_{eff}. In the following we discuss $\beta = 0.5\beta_{eff}$. In figure 4 the splitting of the rocking angle between two twin related domains on a (001) surface is shown as function of temperature. The line represents the expected temperature evolution for a 2–4–6 Landau potential of a one-component order parameter including quantum saturation, $G = 1/2A\theta_s(\coth(\theta_s/T) - \coth(\theta_s/T_c))Q^2 + 1/4BQ^4 + 1/6CQ^6$, [37, 38]. The numerical values of the Landau potential are $\theta_s = 52(2)$ K, $B/A = 10(1)$ K, $C/A = 50(2)$ K, $T_c = 104$ K. The comparatively small value of B/A shows that the transition appears to be close to a tricritical point. No attempt was made at this point to identify possible deviations

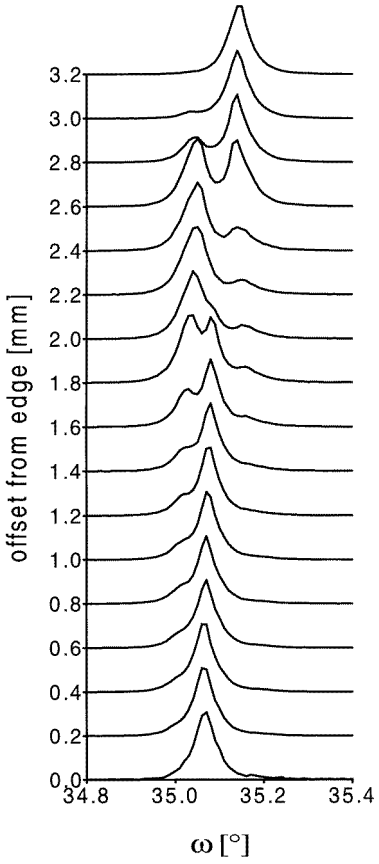

Figure 2. Typical example for rocking curves at room temperature. The x-ray beam is scanned over the sample surface showing bending and warping in the middle of the crystal while the two ends remain reasonably planar.

between the experimental data and this prediction of Landau theory at low temperatures (e.g. near 40 K). The deviations near the transition point in this surface sensitive experiment are similar to those observed previously in the bulk [2–4, 16, 17].

From the widths of the diffraction peaks at the respective ω_{max} of the rocking curves (i.e. intensity versus θ) we estimate the correlation lengths of the two domain systems using the Scherrer approximation [25]. The size of the domains depends only weakly on temperature or uniaxial stress with a characteristic length of '*a*' domains at 2000 Å while the '*c*' domains are much smaller with a characteristic length of 700 Å.

3.2. {*100*} *orientation*

The temperature dependent measurements on the same crystal under various uniaxial pressures reveal a weaker dependence of this surface layer on small external stresses than the {110} sample. At $T < T_c$ the reflection 004 is split at all stresses into 400 and 004 due to twin domain formation close to the surface. In figure 5 the same intensity ratios as in figure 3 are plotted as a function of temperature for three different stresses. The

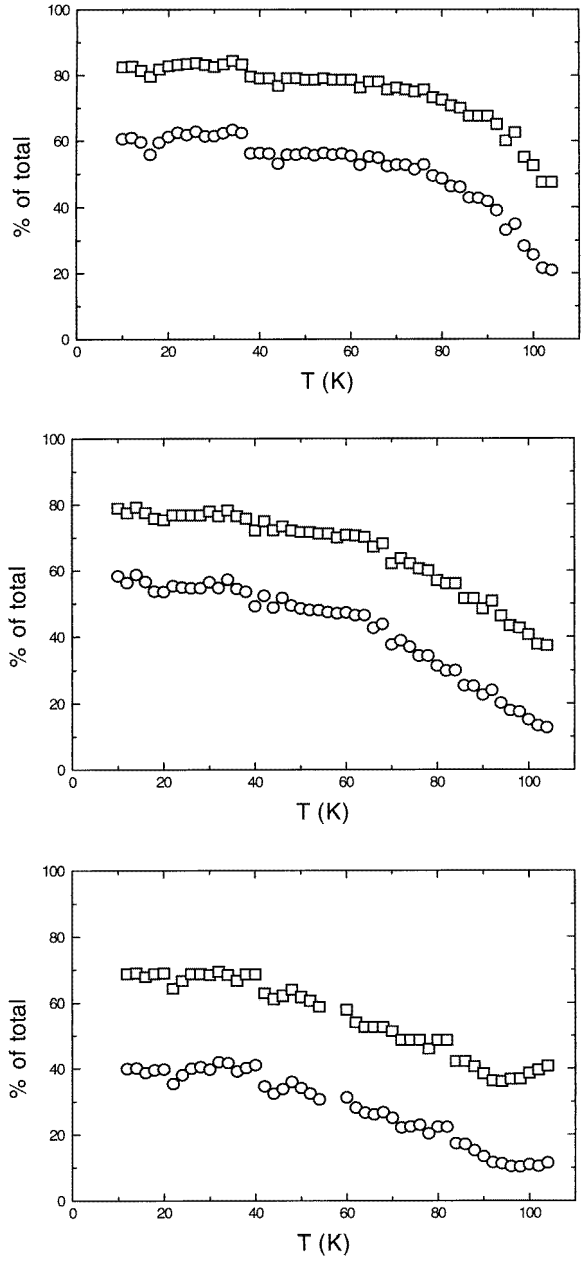

Figure 3. Temperature evolution of the population of '*c*' domains on the (001) surface with stress applied along [110] (see figure 1). Squares indicate the total population while circles show the fraction of '*c*' domains aligned within 0.01° perpendicular to the surface (top: $p = 200$ Pa, middle: $p = 400$ Pa, bottom: $p = 600$ Pa).

intensity ratios are quite constant at low stresses and do not vary much with temperature up to ca 60 K. At higher temperatures the volume ratio begins to deviate from this value indicating that the domain distribution changes and shows a bias towards '*a*' domains on

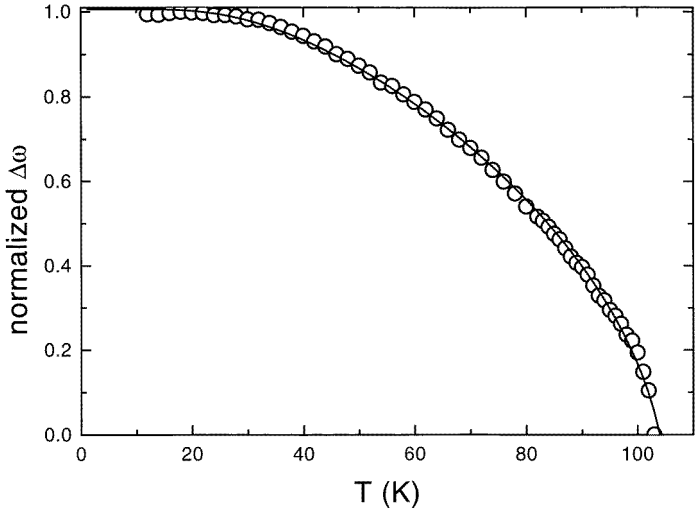

Figure 4. Temperature dependence of the splitting of the rocking angle between two domain orientations. The line is the prediction of a Landau type 2–4–6 potential and quantum fluctuations [37]. The temperature evolution of the near-surface regions is practically the same as observed previously for the bulk.

approaching T_c. At the highest pressure of about 600 Pa a preference of '*a*' domains is seen at low temperatures that increases further when the temperature approaches T_c. Under repeated cooling, we find the domain population changes reversibly in this sample.

4. Discussion

4.1. Domain orientations

The integrated intensity of a diffraction peak (i.e. the maximum height of the ω rocking curve) is a measure for the diffracting volume from domains in one particular orientation. For a totally random distribution of small domains the ratio (I_{004}/I_{total}) is 1/3 while larger (smaller) values indicate a higher population of '*c*' ('*a*') domains.

Stress parallel to [100] is a bias which favours one of the (shorter) *a*-axes of the tetragonal phase to be parallel to [100] [26]. The (longer) *c*-axis has still two possible orientations, namely along the [010] and the [001] direction. Therefore, perpendicular to the applied stress, one expects a statistical distribution of domains at low temperatures with a 50% population of '*c*' domains.

Stress along [110], on the other hand, favours directly a domain orientation with the *c*-axis parallel to the [001] direction. Hence, on increasing stress the sample is expected to transform into a monodomain crystal (i.e. the population of '*c*' domains approaches 100%) although the stresses needed to achieve this state may exceed our experimental range [27–29]. The domain orientation is additionally biased by surface effects [30].

Applied additional external stress parallel to [100] leaves a distorted crystal with the *c*-axis of the low-temperature phase still in two possible orientations if the surface effect of slightly shortening the lattice constant is equal in both the [010] and the [001] direction. We find that this effect is small for flat surfaces (but probably not for curved surfaces). In our experiment on {100} oriented samples we observe a ca 50% population of '*c*' domains

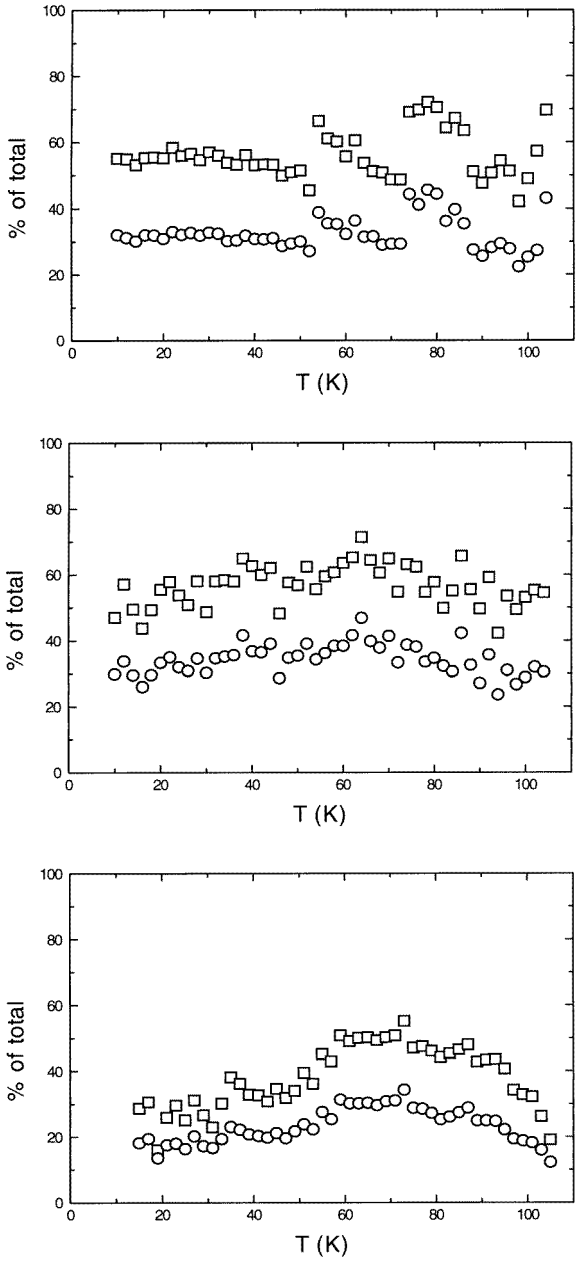

Figure 5. Population of '*c*' domains for a sample with {100} faces. Squares indicate the total population, circles represent the population of '*c*' domains aligned within 0.01° perpendicular to the surface (top: $p = 0$ Pa, middle: $p = 00$ Pa, bottom: $p = 600$ Pa).

at low temperatures and stresses (figure 5). At temperatures $T \approx T_c - 30$ K the domain pattern changes upon heating. An increasing number of '*a*' domains appear under external stress of 600 Pa while the dominance of '*c*' domains remains for all other stresses. For high stresses we find a change of population densities with changing temperature. This can

be understood if the surface area which contributed to the diffraction signal contains only a small number of domains. Any rapid movement of a wall between domains will strongly change the volume contribution of the two possible types of domain. The dominance of '*a*' domains under uniaxial stress can, in a statistical sense, be accidental if only a few large domains occur. Under all smaller stresses the ratio between '*a*' and '*c*' domains is roughly unity which is much lower than the value for a random distribution. The '*a*' domains are well aligned with respect to the surface and show no broadening in the ω-direction. The '*c*' domains, on the other hand, show a very broad rocking curve in ω. Its origin may be a wider angular spread of the orientation of the *c*-axis by 1° rather than size broadening of the '*c*' domains perpendicular to the surface (which appears in the 2θ direction). Alternatively, the wider ω distribution of the diffraction signal may indicate a small domain size of '*c*' domains parallel to the surface. A typical scenario could be a dense array of c-oriented needle domains reaching from the surface into the bulk. The characteristic size of the '*c*' domains within the surface would then be ca 150 Å.

The {110} sample also shows the expected dominance of '*c*' domains near the (001) surface (figure 3). The angular spread of the c axis with respect to the surface is again $\approx 1^\circ$ while the '*a*' domains are well aligned. The dominance of '*c*' domains near the (001) surface can be visualized by the way the octahedra rotation appears in the tetragonal phase. Any rotation around an axis perpendicular to the surface (i.e. '*c*' domains) does not change the shape of the actual surface layer and appears to be energetically favourable. In contrast to such rotations, '*a*' domains require rotation axes which are oriented parallel to the surface. This requires that the surface layer is distorted in a tetragonal manner: it is stretched along the tetragonal *c*-axis and compressed along the *a*-axis. Furthermore, the rotation leads to a corrugation effect in the surface with every second row of oxygen atoms above the original, cubic surface layer while other oxygen positions shift below the original surface. From this difference between the geometrical surface distortion of '*a*' and '*c*' domains the observed dominance of '*a*' domains can be rationalized.

Increasing uniaxial stress on the {110} sample is expected to increase the dominance of the '*c*' domains perpendicular to the stress axis. This is not observed at the small (001) surface. We find that the number of '*a*' domains increases with increasing external stress which might be related to the fact that the stress field might damage the surface which is measured by the x-ray beam. Another interpretation of this curious observation is that the bulk of the material has indeed transformed into a coarse domain structure with a dominance of '*c*' domains perpendicular to the stress axis. This elongates the crystal plate along the *c*-axis and produces additional stress fields close to the edges of the plate. Compensating the elongation in one direction one might expect '*a*' domains in an orthogonal orientation to dominate at the edges of the plate. Increasing uniaxial stress will then increase the number of '*a*' domains in this part of the sample. There has been no direct observation of the domain structures using topographical methods. The interpretation of our experimental findings parallels the analysis of the twin domain formation in Er doped LaP_5O_{14} by Hu *et al* [31].

4.2. Characteristic length scales

The analysis of the characteristic lengths of the two domain systems in sample {110} illustrates the different behaviour of '*a*' and '*c*' domains with temperature and pressure. The '*c*' domains are much smaller perpendicular to the surface than the '*a*' domains.

The domain size of '*c*' domains is sensitive to both temperature and stress. The reason for this becomes obvious if one recalls the structural changes connected with the domain

formation. To change the correlation between '*a*' domains is much more difficult because it involves the simultaneous rotation of octahedra in opposite directions across a twin boundary. The domain boundary can be described as a twin wall with rather high wall energies [32]. In contrast, the '*c*' domains are more weakly correlated because their different orientations are due to a simple rotation of octahedra around the *c*-axis. Changes in the clockwise → anti-clockwise rotation sequence are equivalent to the formation of anti-phase boundaries parallel to the crystal surface. Our results show that there are many more anti-phase boundaries than twin boundaries present in the near-surface regions. Furthermore, the anti-phase boundaries appear and disappear in a reproducible fashion when the temperature and stress conditions of the sample are changed. No criticality is seen in the domain size for $T \to T_c$.

4.3. Order parameter behaviour

The order parameter evolution is dominated by large twin domain structures which form immediately upon cooling to $T \lesssim T_c$. Inside each domain, the tilt axes of the octahedral rotation are all parallel (i.e. $n = 1$). Fine-scale anti-phase boundaries are evident from the small effective size of the '*c*' domains. We find no indication for large volume contributions for flips of the tilt axis or tumbling motions which exceed the mosaic spread of 1°.

There is no significant diffuse scattering close to the Bragg peaks which could indicate that orientational disorder of the rotation axis plays a role in the temperature evolution of the order parameter. From our experimental observation the following picture of the tetragonal phase emerges: the tetragonal phase shows large twin domains and finer anti-phase domains. The size of anti-phase domains is much bigger than the dimensions of the crystallographic unit cell. The order parameter evolution inside each domain on cooling is the increase of the rotation angle and the simultaneous change of the shape of the octahedra. More importantly, it has nothing to do with any reorientational flips of rotation axes which is required if the order parameter behaviour is described within a Heisenberg model. Instead, the tetragonal phase is best described as displacive and antiferroelastic.

The question arises then why an empirical order parameter exponent $\beta \approx 0.4$ is found between T_c and $T_c - 15$ K. Traditionally, this value is correlated with some Ising or Heisenberg type behaviour in this temperature interval while classic mean field behaviour is expected at lower temperatures (see [24] for an illuminating review). Our results do not support this view. The results in figure 4 are analysed in a most simple Landau type mean field approach. They show that the order parameter behaviour follows over a wide interval a near-tricritical temperature dependence. The classic value $\beta = 0.5$ is, in this case, observed only in a very small interval near T_c which is not accessible in our experiment. In a separate paper we shall show that other experimental results can well be analysed using the same Landau-type expression for the Gibbs excess free energy.

We may now compare $SrTiO_3$ with another, archetypal antiferroelastic material, namely $Pb_3(PO_4)_2$–$Pb_3(AsO_4)_2$ [33–35]. This material shows a slightly first-order transition for P-rich components, a tricritical point at an intermediate composition, and a second-order transition for As-rich material. It also shows orientational flip motions at $T > T_c$ and seemingly 'exotic' values of β close to T_c. In $Pb_3(PO_4)_2$, dynamic reorientational flips are found at $T \leqslant T_c$ but not for any material containing As (or significant amounts of impurities). In all these cases, the temperature evolution of the order parameter follows mean field behaviour with Landau potentials similar to $SrTiO_3$.

We now emphasize the unusual behaviour of $SrTiO_3$ as compared with other improper ferroelastic material [32]. While the latter also form domain structures at temperatures

just below T_c, the mesoscopic domain pattern changes little under cooling (besides the sharpening of the domain walls) [23, 24]. This behaviour is also observed in stress free {100} samples of $SrTiO_3$. In {110} samples the near-surface domain patterns are almost independent of temperature in a small interval below T_c. At lower temperatures, the domain population in {110} samples is strongly temperature dependent; only below ca 45 K does this temperature evolution disappear. At the same temperature the temperature dependence of the order parameter levels off because quantum saturation sets in [35, 36]. This means that in the {110} sample, the domain pattern changes strongly with changes of the static order parameter. This type of behaviour has not, to the best of our knowledge, been observed in other ferroelastic or anti-ferroelastic materials.

We have also observed $\beta = 0.5$ for $T \rightarrow T_c$ in a strongly biased {110} sample. It appears that in this experiment large surface bias has effectively eliminated all secondary order parameter components so that a pure $n = 1$, mean field behaviour is observed over the full temperature interval (as far as it was experimentally accessible). This observation is in agreement with earlier results of specific heat measurement where second-order, mean field behaviour was found for a stressed sample [10]. Further work on {110} samples under high uniaxial stress would be desirable to see if also the bulk order parameter can be squeezed into a classic mean field behaviour as might be expected also from the previously observed crossover behaviour [7, 9].

References

[1] Unoki H and Sakudo T 1967 *J. Phys. Soc. Japan* **23** 546
[2] Cowley R A, Buyers W J L and Dolling G 1969 *Solid State Commun.* **8** 181
[3] Shirane G and Yamada Y 1969 *Phys. Rev.* **177** 858
[4] Müller K A and Berlinger W 1971 *Phys. Rev. Lett.* **26** 13
[5] Courtens E 1972 *Phys. Rev. Lett.* **29** 1380
[6] Aharony A and Bruce A 1979 *Phys. Rev. Lett.* **42** 462
[7] Stokka S and Fossheim K 1982 *Phys. Rev.* B **25** 4896
[8] Chang T S, Holzrichter J F, Schawlow A L and Imbusch G F 1969 *Bull. Am. Phys. Soc.* **14** 1158
[9] Müller K A and Berlinger W 1975 *Phys. Rev. Lett.* **35** 1547
[10] Gallardo M C, Jiménez J, del Cerro J and Salje E K H 1996 *J. Phys.: Condens. Matter* **8** 83
[11] Darlington C N W and O'Connor D A 1976 *J. Phys. C: Solid State Phys.* **9** 3561
[12] Andrews S R 1986 *J. Phys. C: Solid State Phys.* **19** 3721
[13] Nelmes R J, Hatton P E and Vass H 1988 *Phys. Rev. Lett.* **60** 2172
[14] McMorrow D F, Hamaya N, Shimomura S, Fujii Y, Kishimoto S and Iwasaki H 1990 *Solid State Commun.* **76** 443
[15] Shirane G, Colwey R A, Matsuda M and Shapiro S M 1993 *Phys. Rev.* B **48** 15 595
[16] Neumann H B, Rütt U, Schneider J R and Shirane G 1995 *Phys. Rev.* B **52** 3981
[17] Hirota K, Hill J P, Shapiro S M, Shirane G and Fujii Y 1995 *Phys. Rev.* B **52** 13 195
[18] Salje E K H 1995 *Phase Transitions* **55** 37
[19] Salje E K H and Chrosch J 1996 *Ferroelectrics* **183** 85
[20] Chrosch J and Salje E K H 1996 *Ferroelectrics* **187** 1
[21] Wruck B, Salje E K H, Zhang M, Abraham T and Bismayer U 1994 *Phase Transitions* **48** 135
[22] Chrosch J and Salje E K H 1994 *Physica* C **225** 111
[23] Hayward S A, Chrosch J, Salje E K H and Carpenter M A 1996 *Eur. J. Min.* **8** 1301
[24] Locherer K R, Hayward S A, Hirst P J, Chrosch J, Yeadon M, Abell J S and Salje E K H 1996 *Phil. Trans. R. Soc.* A **354** 2815
[25] Warren B E 1996 *X-ray Diffraction* (Reading, MA: Addison-Wesley)
[26] Cowley R A 1996 *Phil. Trans. R. Soc.* A **354** 2799
[27] Burke W J and Pressley R J 1971 *Solid State Commun.* **9** 191
[28] Uwe H and Sakudo T 1976 *Phys. Rev.* B **13** 271
[29] Chang T S, Holzrichter J F, Imbusch G F and Schawlow A L 1970 *Appl. Phys. Lett.* **17** 254
[30] Houchmandzadeh B, Lajzerowicz J and Salje E K H 1992 *J. Phys.: Condens. Matter* **49** 9779

[31] Hu Z W, Jiang S S, Huang P Q, Huang X R, Feng D, Wang J Y and Li L X 1994 *Appl. Phys. Lett.* **64** 55
[32] Salje E K H 1990 *Phase Transitions in Ferroelastic and Co-elastic Crystals* (Cambridge: Cambridge University Press)
[33] Salje E K H, Graeme-Barber A, Carpenter M A and Bismayer U 1993 *Acta Crystallogr.* B **49** 387
[34] Salje E K H, Devarajan V, Bismayer U and Guimaroes D M C 1983 *J. Phys. C: Solid State Phys.* **16** 5233
[35] Salje E K H and Devarajan V 1981 *J. Phys. C: Solid State Phys.* **14** L1029
[36] Salje E K H, Wruck B and Thomas H 1991 *Z. Phys.* B **82** 399
[37] Salje E K H, Wruck B and Marais S 1991 *Ferroelectrics* **124** 185